Astronomy & Astrophysics manuscript no. jet˙1
September 14, 2011

Observations of multiple ejecta and oscillations associated with a large blowout solar jet

R. J. Morton[1], A. K. Srivastava[2,1], & R. Erdélyi[1]

[1]Solar Physics and Space Plasma Research Centre (SP^{2}RC), University of Sheffield, Hicks Building, Hounsfield Road, Sheffield S3 7RH, UK,
[2] Aryabhatta Research Institute of Observational Sciences (ARIES), Nainital 263129, India
email:[r.j.morton, robertus]@sheffield.ac.uk

Received /Accepted

ABSTRACT

Aims. A variety of periodic phenomena have been observed in conjunction with large solar jets. We aim to find further evidence for periodic behaviour in solar jets and determine what the periodic behaviour can tell us about the excitation mechanism and formation process of the large solar jet.
Methods. Using the 304 Å (He-II), 171 Å (Fe IX), 193 Å (Fe XII/XXIV) and 131 Å (Fe VIII/XXI) filters onboard the Solar Dynamic Observatory (SDO) Atmospheric Imaging Assembly (AIA), we investigate the intensity oscillations associated with a solar jet.
Results. Evidence is provided for multiple magnetic reconnection events occurring between a pre-twisted, closed field and open field lines. Components of the jet are seen in multiple SDO/AIA filters covering a wide range of temperatures, suggesting the jet can be classified as a blowout jet. Two bright, elongated features are observed to be co-spatial and co-temporal with the large jet, appearing at the jet's footpoints. Investigation of these features reveal they consist of multiple plasma ejections. The rate of recurrence of the ejecta displays (quasi) periodic behaviour (50 s), with estimated initial temperatures of the plasma $\sim$ 0.1 MK and rise velocities of $40 - 150$ kms^{-1} along the open field lines. Due to the suggestion that the large jet is reconnection driven and the observed properties of the ejecta, we further propose that these ejecta events are similar to type-II spicules. The multiple, fast, hot ejections may be evidence for 'nano-flare' storms in the chromosphere. We also report for the first time the presence of intensity oscillations in large solar jets, mainly associated with the plasma curtain. A wave with a period of 300 s is also present, which we interpret as the slow magnetoacoustic mode. The sound speed for the mode is obtained and the corresponding plasma temperature is estimated using magneto-seismology. Possible explanations for its excitation in terms of jet dynamics and the response of the transition region are discussed.

1. Introduction

Solar jets are relatively short lived, transient, common features observed often at the solar limb. Their presence demonstrates the active nature of the underlying solar atmosphere suggesting ubiquitous, fine-scale explosive magnetic events (e.g., Schrijver et al., 1998; Moore et al., 2011). The term solar jets covers a wide range of plasma ejection events that have been observed over the last century, including Hα surges (Newton, 1934), spicules (Secchi, 1877 or e.g., Beckers, 1972 and references within), type-II spicules (De Pontieu et al., 2007a), macrospicules (Bohlin et al., 1975), UV jets (Brueckner & Bartoe, 1983), EUV jets (Budnik et al., 1998) and X-ray jets (Shibata et al., 1992). There is some suggestion that these events may all be closely related but no firm evidence has yet been presented to establish this. Large solar jets may launch plasma hundreds of Mm into the solar atmosphere where the plasma can, sometimes, be seen to exhibit a torsional/helical motion during the jets rise. The driving mechanism behind these various jets is also yet to be firmly established but the height and speed of the large jets has lead to the proposition of a mechanism involving magnetic reconnection (e.g. Yokoyama & Shibata, 1995, 1996). Jet models often revolve around the emergence of magnetic flux interacting with the existing magnetic field or the motion of existing magnetic fields (Shibata et al., 1992; Moore et al., 2010). Shibata et al. (2007) suggests that varying the heights of the reconnection may give rise to the range of jets observed. Increased spatial resolution and the ability for multi-wavelength analysis of these large jets (e.g., Liu et al., 2011) should provide some answers to the excitation mechanisms and determine the main differences, if any, between the various reported jet phenomena. Some differences between large solar jets has been defined by Moore et al. (2010), who suggest two categories, namely, 'standard' and 'blowout' jets. Standard jets fit the emerging flux-open field reconnection model mentioned earlier, and emission is mainly seen in X-rays. On the other hand, blowout jets begin as standard jets but the emerging flux erupts during the formation of the standard jet. This results in the presence of a mutli-thermal jet, with chromospheric and transition region material ejected in addition to the X-ray jet.

The importance of studying jet phenomena is highlighted by the current and considerable interest in type-II spicules. The reported properties of the type-II spicules suggest they are fast moving ($50 - 150$ kms^{-1}), apparently short lived ($45 - 60$ s) jets that are heated as they rise from the chromosphere, where they are seen in Ca II filters ($T \sim 0.01 - 0.02$ MK), to the corona, with temperatures possibly reaching 2 MK. The interest is due to the suggestion that they may play a role in the heating of the quiet Sun, acceleration of the solar wind and maintaining the mass balance in the corona (see, e.g., De Pontieu et al., 2007b, 2009; McIntosh & De Pontieu, 2009b,a; De Pontieu et al., 2011 and Tian et al., 2011). The type-II spicules are believed to be ex-

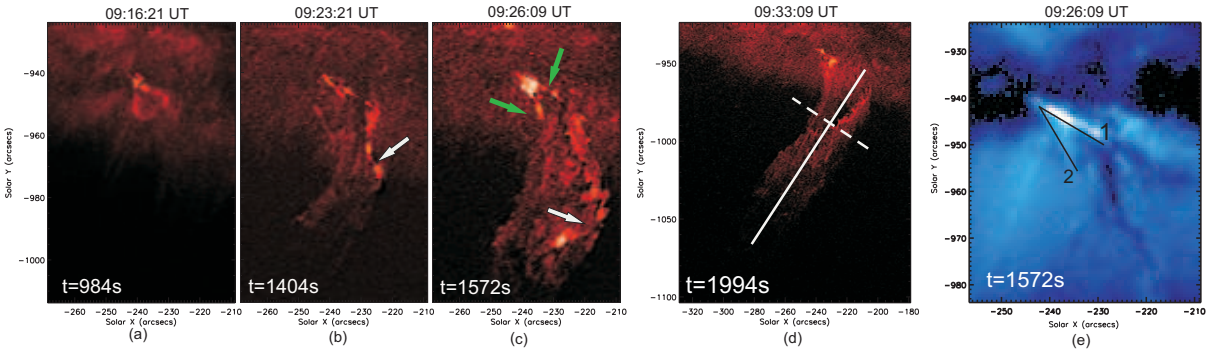

Fig. 1: Images from the AIA 304 Å channel. All times in seconds are given as times after 9:00 UT on 20 January 2011. (a) A small-scale loop or arcade brightening at the base of the solar jet. (b) The arrow shows the twisted magnetic field highlighted by bright plasma. (c) The onset of helical motion in the plasmas curtain. The white arrow shows the position where the whip-like effect is seen. The green arrows point-out the two, bright elongated features either side of the jet at its footpoints. (d) An image of the full jet close to its maximum height. The solid white line shows the position of the cross-cut in Fig. 2. The dotted line is the position of the cross-cut in Fig. 3. (e) Shows the cross-cuts (black lines) placed along the bright elongated features at the footpoint of the jet in AIA 171 Å. The image also shows clearly the dark filament thought to be an ejected magnetic loop (or arcade).

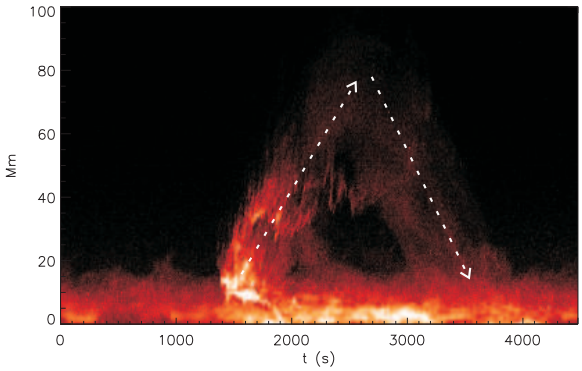

Fig. 2: Time-distance plot from the cross-cut along the jet axis shown in Fig. 1d, demonstrating the evolution of the plasma curtain. The arrows mark out the paths used to calculate the average up-flow and down-flow speeds of the plasma curtain.

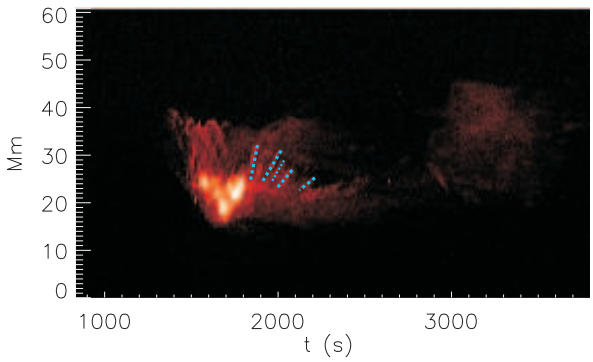

Fig. 3: Time-distance plot from the cross-cut across the jet shown in Fig. 1d. The blue dashed lines highlight the some of the signatures of the torsional motion of the plasma curtain.

cited by reconnection events in the lower solar atmosphere and have been identified in advanced simulations of chromospheric dynamics (Martínez-Sykora et al., 2011).

Observations of the supposedly different jet phenomena have been identified in a singular event. Sterling et al. (2010) report observing bright, fast moving jet features around 20 Mm in length in Ca II (i.e. at chromospheric temperatures, $T \sim 0.01 - 0.02$ MK), at the footpoints of a larger 'blowout' solar jet seen in EUV and soft X-rays. The authors also note the jets observed in Ca II have rise speeds similar to type-II spicules but last for 5 minutes, much longer than previously reported type-II events. However, the observations offer no insight into how these Ca II jets are generated.

Recently, the presence of waves has begun to be observed in observations of solar jets. The study of wave phenomena in the solar atmosphere has received increased attention over the last two decades. This is partly due to improved spatial and temporal resolution on both space- and ground-based telescopes, paving the way for the new and expanding field of solar magneto-seismology (Uchida, 1970; Roberts et al., 1984; Erdélyi, 2006a,b) which exploits observed wave phenomena to determine hard to measure or otherwise unmeasurable plasma parameters, e.g., the magnetic field strength of the individual magnetic waveguides (see, e.g., Banerjee et al., 2007; Andries et al., 2009; De Moortel, 2009; Ruderman & Erdélyi, 2009; Taroyan & Erdélyi, 2009; Wang, 2011 for reviews of waves in the solar atmosphere and how to exploit them for diagnostic purposes). Advances in ground-based technology has led to the development of high resolution and high cadence instruments that have allowed the first, and yet undisputed, direct detections of linear Alfvén (Jess et al., 2009) and sausage (Morton et al., 2011a) waves.

The magnetic reconnection models predict that some form of wave phenomena is generated by a reconnection event. Two-dimensional numerical simulations by Yokoyama & Shibata (1996) demonstrate the presence of non-linear slow and fast modes due to the reconnection. Pariat et al. (2009) predicts the presence of kink motions propagating along the field lines surrounding a rotating, closed magnetic region. The kink motions

are assumed to be due to a kink instability of the magnetic region before reconnection occurs.

The most visible, and consequently most reported, sign of waves in the large jets is torsional/helical mode that is due to the untwisting of the jet as it rises (e.g., Shimojo et al., 1996; Pike & Mason, 1998; Patsourakos et al., 2008; Liu et al., 2009; Kamio et al., 2010). This feature is possibly due to the relaxation of a twisted field line which has reconnected with an open coronal field line (Shibata & Uchida, 1985; Pariat et al., 2009). However, the helicity is also reported in spicules and macro-spicules, e.g. Zaqarashvili & Erdélyi (2009); Curdt & Tian (2011), with spicules (type-I) generally thought to be driven by waves (De Pontieu et al., 2004). Transverse motions along the jet axis have also been reported in both smaller jets, i.e., type-I spicules (e.g., Kukhianidze et al., 2006, De Pontieu et al., 2007b, He et al., 2009), and large jets (Cirtain et al., 2007; Vasheghani Farahani et al., 2009; Morton et al., 2011b). Recent observations and simulations in Scullion et al. (2011) also find waves propagating *along* the transition region due to the interaction of a jet with the transition region.

In the following work, we investigate wave phenomena associated with a large solar jet. Plasma with a range of temperatures is seen to be ejected into the corona. Two, bright elongated features are observed at the footpoints of the large jet and are seen to consist of fast moving, bright ejecta. The measured velocities ($40 - 150$ kms^{-1}), curved paths seen in time-distance plots, lifetimes and apparent temperatures ($T \sim 0.1$ MK) of the bright ejecta that make up the elongated features are very similar to the previously reported features of type-II spicules. Further periodic intensity disturbances are also seen throughout the large jet, with seismology suggesting the oscillations are connected to the material that makes up the plasma curtain of the large jet seen in 304 Å. This wave behaviour is in conjunction with a propagating transverse kink wave seen in a cool filament ejected with the large jet (Morton et al., 2011b). These observed waves allow us to draw conclusions, along with observational evidence, that the large jet was excited by a low atmosphere (possibly chromospheric) reconnection event.

2. Observations

The observations began at 09:00 UT on 20 January 2011 and last an hour and a quarter till 10:15 UT, on the south west limb using the Solar Dynamic Observatory (SDO) Atmospheric Imaging Assembly (AIA) (Lemen et al., 2011). SDO/AIA has a spatial resolution of ~0.6 arcsec per pixel (435 km) and a cadence of ~12 s. The large solar jet (Fig. 1d) was observed clearly in the 304 Å and 171 Å spectral lines close to the southern polar coronal hole. We also see the jet event partially in higher temperature lines, but will only use information from the 193 Å and 131 Å filters. The time series were obtained from the SSW cutout service and had already been corrected for flat-field, despiked and co-aligned. Some aspects of the jet have already been studied in Morton et al. (2011b).

The observed evolution of the jet is as follows. A region, approximately 11000 km is diameter, close to the limb is seen to undergo a brightening at 09:15 UT in 171 Å. In 304 Å we simultaneously see 3-4 small patches of bright emission, followed by the appearance of a bright loop or arcade seen in both channels (Fig. 1a). The emission is seen to increase in the left-hand leg of the loop and then fills the loop in ~ 60 s, suggesting heated plasma flows along the loop.

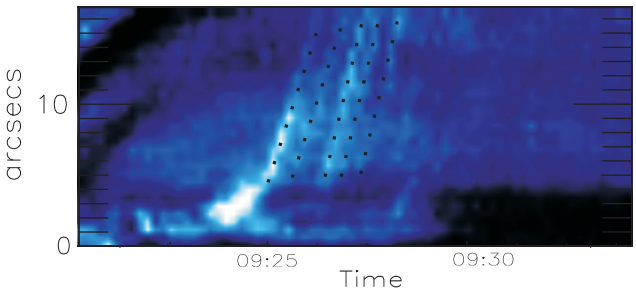

Fig. 5: A zoom of the time-distance plot in Fig. 4 for the cross-cut 2 in 171 Å. The paths of the multiple bright ejecta are highlighted with dotted black lines.

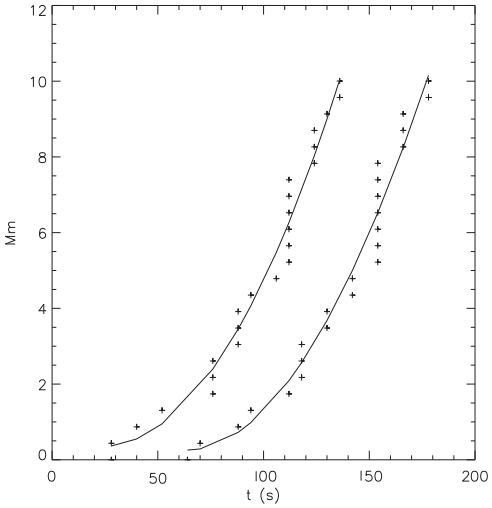

Fig. 6: Examples of the tracks made by the bright ejecta seen in the time-distance plots. The crosses represent the points of maximum intensity along the track and the solid line is a cubic polynomial fitted to the data points.

After the loop/arcade brightening, plasma begins to rise from the left hand side of the loop in 304 Å. The plasma rises above the surrounding spicular material obscuring the loop from view. Approximately 250 s after the loop has disappeared, the dark plasma has formed a collimated jet and brighter plasma starts to travel along the edges of the jet. The bright plasma appears to highlight twisted magnetic field lines, seen by the bright 's' shapes (Fig. 1b). As the plasma rises higher, the upper portion of the bright twisted field lines fade and two bright, elongated features remain at the base of the jet (Fig. 1c and e). These features exist while plasma is being ejected into the atmosphere; however, once plasma ejection has diminished they fade from view.

The jet has a different appearance in the 304 Å channel compared to that seen in the 171 Å, 193 Å and 131 Å. The jet is the most visible in 304 Å, where a significant amount of plasma is seen to be launched into the solar atmosphere to a height of ~ 100 Mm. This material makes up what is referred to as the plasma curtain. The ejected plasma flows outwards, at an angle

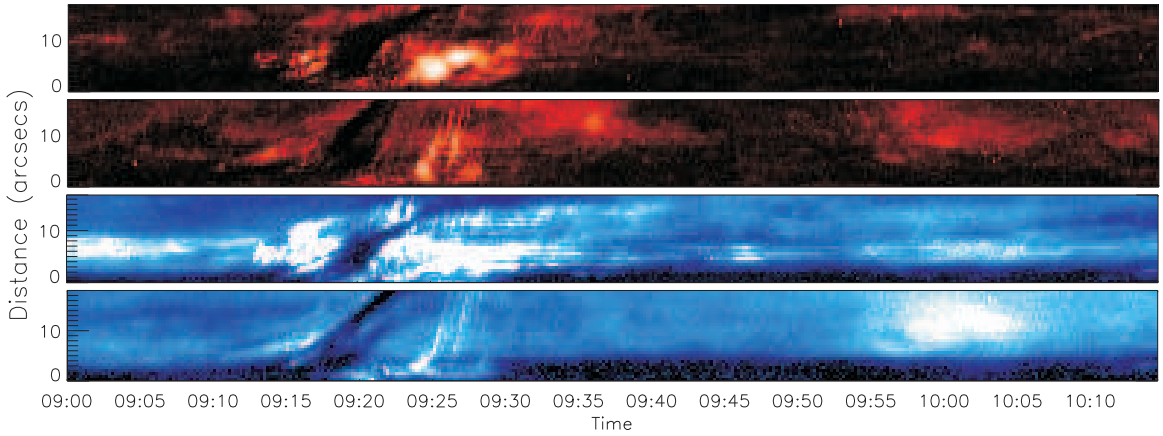

Fig. 4: The time-distance plots for the cross-cuts placed along the bright, elongated features at the base of the jet. The top two panels shows the cross-cuts obtained 1 and 2 for 304 Å. The bottom two panels show the cross-cuts 1 and 2 obtained for 171 Å.

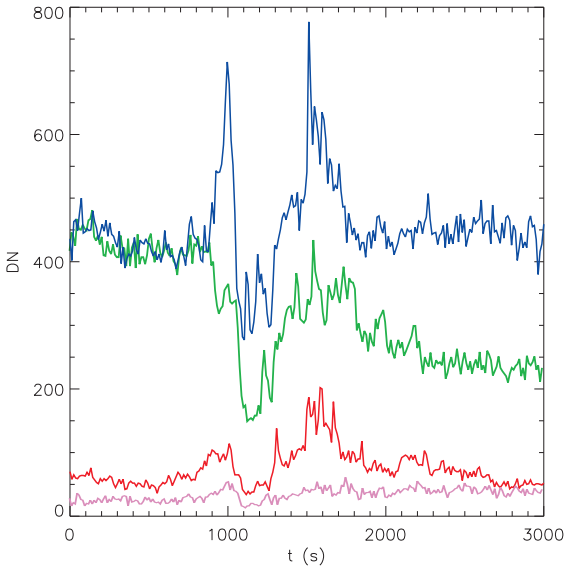

Fig. 7: The flux as a function of time for the pixel located at 10 arcseconds along bottom bright feature in Fig. 4. The red, blue, green and purple lines corresponds to the 304 Å, 171 Å, 193 Å and 131 Å time series, respectively. The time series are shown from 09:00 UT to 09:48 UT.

to the normal from the surface (from left to right in Fig. 1c). At a height of ∼ 18 Mm above the jet base, a whip-like motion of the the jet occurs sending the out-flowing plasma in the opposite direction (right to left), giving the plasma curtain a helical motion (Fig. 1c). The majority of the plasma is ejected between 09:15 UT and 09:35 UT. At a later time, a portion of the ejected material is also seen to return to the surface. A cross-cut along the axis of the jet is made and an time-distance plot of the jet rise is obtained (Fig. 2). Bright, outward flowing plasma can be seen to be initially ejected in bursts at ∼ 1400 s after the observations begin. An average value for the outwards velocity of the plasma during the rise phase is 72 kms^{-1}. The plasma curtain cools and begins to fall, with an average speed of 82 kms^{-1}, giving the observed parabolic profile. Another cross-cut (see, Fig. 1d for cross-cut position) is placed perpendicular to the jet axis at around 33 Mm above the jet footpoint. The corresponding time-distance plot is shown in Fig. 3 . The onset of helical motion in the plasma curtain can be seen at 1700 s, highlighted by the diagonal lines in the plot.

In 171 Å, 193 Å and 131 Å we see much less material being ejected. The bright elongated features are still present along with a dark filament. The properties of this dark filament are explored in detail in Morton et al. (2011b). The filament is seen to rise from the jet excitation site and is found to have a temperature of $2 - 3 \times 10^4$ K. This suggests the filament is the remnant of a chromospheric magnetic loop (or arcade) that has been ejected. The filament is mainly obscured from sight in the 304 Å channel by the hotter plasma that makes up the plasma curtain. The plasma curtain is not as distinct in the 171 Å, 193 Å and 131 Å as coronal emission dominates the channels. In 193 Å and 131 Å only the bright, elongated feature (labeled 1) closest to the solar surface is clearly visible, the other feature (2) is much fainter in comparison.

The bright loop/arcade and the twisted field lines suggest a scenario where twisted, emerging flux has reconnected with open field lines and heated plasma flows along the open lines. This scenario has been suggested previously for the formation of large jets (Shibata et al., 1992) and preliminary studies of this scenario are being carried out with numerical simulations (e.g., Pariat et al., 2009). However, we also see cool chromospheric material ($T \sim 0.03$ MK) in the form of the dark filament and the plasma curtain in 304 Å which is probably at transition region temperatures (estimates for the plasmas temperature via seismology are provided later). This would suggest that we are observing an example of the blowout jet, as suggested by Moore et al. (2010). We note also that the spire, typically associated with plasma heated by the reconnection, is absent from the event.

3. Periodic behaviour in the jet

Now that an overview of the large jet has been given, we proceed to examine certain parts of the blowout jet event in detail. In par-

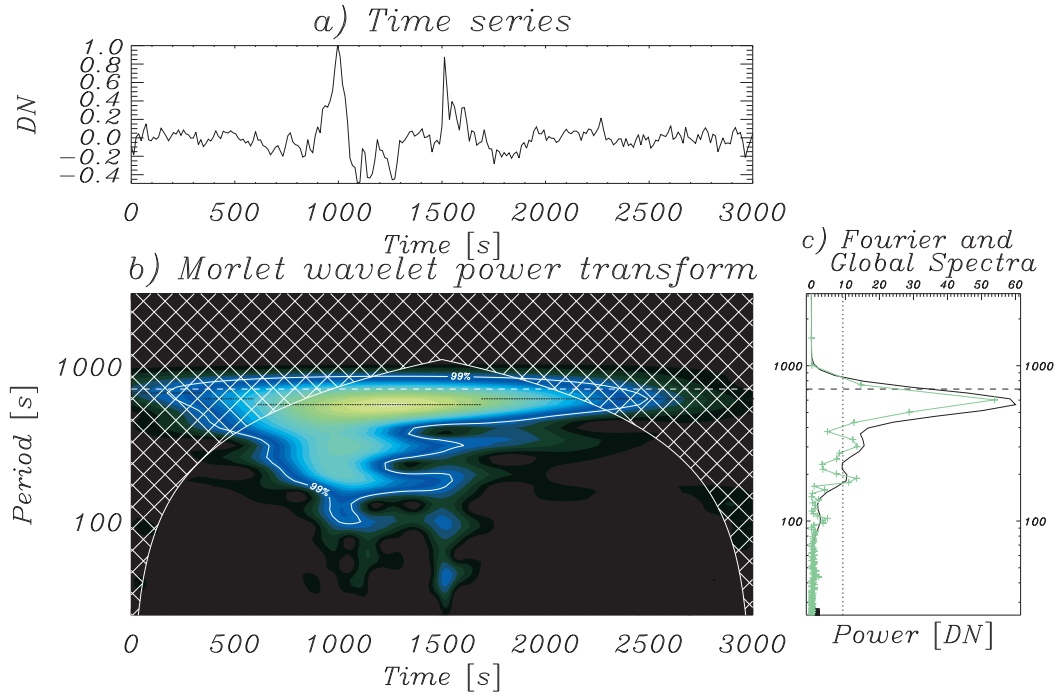

Fig. 8: (a) The time series for the normalised intensity in 171 Å located at 10 arcseconds in cross-cut 2 shown in Fig. 4. The time is measured in seconds from 09:00 UT on 20 January 2011. (b) The wavelet plot for the time series with regions of significant power (> 99%) contoured with the white line. The coloured regions show power above 95%. (c) The Fourier and global powers spectra for the analysed time series.

ticular we are interested in the bright, elongated features seen at the footpoints of the jet. Further, we look for periodic phenomena in the intensity time series of plasma associated with the jet. There are a number reports of periodic phenomena associated with solar jets (Cirtain et al., 2007; Liu et al., 2009; Morton et al., 2011b); however, these observations observe only transverse motions of the ejected jet plasma. To our knowledge, the investigation of intensity perturbations along jets has so far been neglected. We aim to resolve this and demonstrate the potential for magneto-seismology of large solar jets. This will point us towards some interesting ideas about the formation process of the jet and the possible role the transition region plays in this process.

3.1. Periods in bright emission

To begin with, we place cuts (1-pixel wide, 30 pixels in length) along the bright, elongated features seen at the foot-points of the jet (Fig. 1e). The bright features are around 12 Mm in length and separated by 20 degrees, with all the ejected plasma that comprises the jet appearing between these two features. The features last for around 400 s. In Fig. 4 we show the time-distance plots obtained from the cross-cuts placed along the bright features in the 304 Å and 171 Å channels. In both channels and both cuts we see bright emission around 09:15 UT indicating the onset of the jet. This is followed by the rise of cooler plasma followed by the further emission of hotter plasma.

In the cross-cuts placed along the bright feature labeled 2 (Fig. 1e), it can be seen that there are multiple, bright ejections starting at 09:23 UT. The exact number of ejections is hard to distinguish but it appears to be at least 5 occurring within a 300 second time frame. A zoom of the ejecta as seen in the 171 Å cross-cut are shown in Fig. 5 with dotted lines highlighting the paths of the brightest ejecta. It is clear from the time-distance plots that the features are fast moving but the ejections do not have a constant speed. The first ejection is the brightest and it can be seen that, close to the base of the cross-cut, the path is curved, suggesting acceleration. An example of two ejecta paths are shown in Fig. 6. The tracks where obtained by determining the pixels with the greatest value of intensity in the time-distance plots and fitting a cubic polynomial to the obtained points. The velocity was then calculated by differentiating the cubic function. The ejection has an initial speed of 40 kms^{-1} and accelerates to 150 kms^{-1}. The bright material fades as it reaches the end of the cross-cut and the material is not seen to return to the surface. The lifetime of the individual ejecta in both 304 Å and 171 Å filters is between 30 − 120 s. This behaviour is not visible in the cross-cut for the bright feature labeled 1 in Fig. 1e, although the elongated feature appears to be composed of a significant amount of bright material, possibly corresponding to many similar ejections.

Now, because we see multiple ejections we propose to examine the signal to look for periodic behaviour. To begin with we select the pixels located 10 arcseconds along the cross-cut in both 304 Å and 171 Å. The time series for the intensity between 09:00 UT and 09:48 UT of these pixels are shown in Fig. 7. At 1500 s we see 5 large peaks in intensity with a period of ∼ 50 s in both channels. To investigate further, we de-trended the time series and subject it to a wavelet transform, the result is plotted in Figs. 8 and 9. Significant power (contoured at 99%) is found

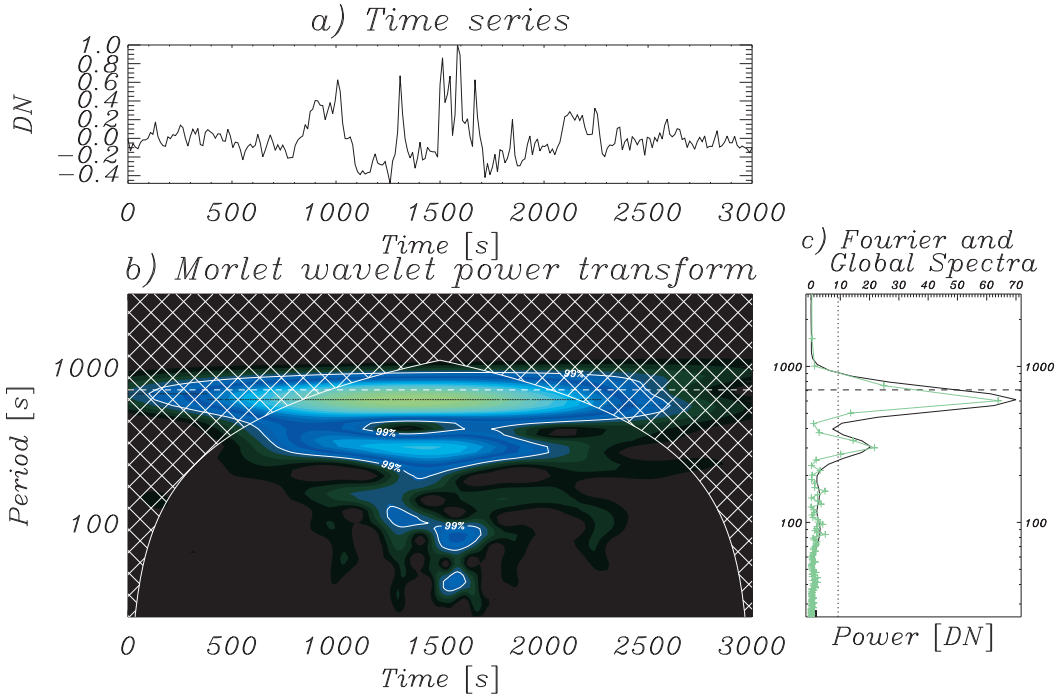

Fig. 9: Similar to Fig. 8 expect the analysed time series is from the 304 Å cross-cut.

in the global spectra at periods of ∼ 200 s and ∼ 300 s in 171 Å (Fig. 8c) and at ∼ 300 s in 304 Å (Fig. 9c). The wavelet transforms (Figs. 8b, 9b) also show the presence of power at 50−100 s periods during the time of the ejecta. However, the power is only contoured above 99% significance in the wavelet of the 304 Å, but int the 171 Å shows power at 95%.

To see the feature we are interested in, we turn to Empirical Mode Decomposition (EMD) (for details see, e.g., Huang et al., 1998; Terradas et al., 2004). The first 4 intrinsic mode functions (IMFs) derived with the EMD for 171 Å are shown in Fig. 10. They correspond to timescales of 50 s, 100 s, 200 s and 300 s, the last two IMFs having the greatest power in the wavelet. Let us concentrate on the first IMF. At 1500 s we see the large peaks in intensity, also observed in the flux time series (Fig. 7). A zoom of this section of the time series is shown in Fig. 11. This signal corresponds to the ejection of the hot material and can be seen to be periodic (or at least quasi-periodic) with a decaying amplitude. The magnitude of the amplitude of the signal is 18% of the median background signal in 171 Å and 41% of the median background signal in 304 Å. Further, the Fast Fourier Transform (FFT) for each pixel in the cross-cut is taken and a Gaussian filter centered on 50 s with a width $f/10$ is applied and the inverse FFT is taken. The results are shown in the top panels of Figs. 12 and 13. This plot provides a somewhat better visualisation of the high speed, up-flowing material, which is clearly seen between 1400 s and 1800 s where the signal is visibly coherent along the cross-cut. Although we cannot see the tracks in Fig. 4 for the cross-cuts along the bright feature 1, the EMD and the FFT technique do reveal that there are the similar, fast moving, up-flowing features with a period of 50 s.

The natural interpretation for a strong, periodic modulation of intensity is the MHD slow mode (most likely the non-linear slow mode due to the large amplitudes). However, there is currently some debate as to whether we can consider these quasi-periodic up-flows as slow modes. Such a discussion is outside the scope of this investigation so we refer an interested reader to the following pieces of work: De Pontieu & McIntosh (2010); Verwichte et al. (2010); Wang et al. (2011).

Now, using further information from the 193 Å and 131 Å filters we try to estimate a temperature for these bright ejecta features. Cross-cuts are placed at the same positions in 193 Å and 131 Å as used for creating the time-distance plots from the 304 Å and 171 Å filters. The bright, high velocity features identified in 304 Å and 171 Å are barely visible. Only very faint streaks can be made out in 193 Å and the streaks cannot be seen in 131 Å. This can be seen in the intensity flux time series in Fig. 7, where multiple, large increases in the intensity are seen in the 304 Å and 171 Å filters around 1500 s but these features are less distinct from the background emission in 193 Å and 131 Å. Using the temperature responses of SDO/AIA given in Lemen et al. (2011), we estimate the temperature of the high, velocity plasma to be $T \sim 0.1 - 0.2$ MK. The 131 Å has a cut-off temperature of $T \sim 0.2$ MK, greater than the other filters used, which have cut-offs less than 0.1 MK. The 304 Å and 171 Å filters have peaks in sensitivity around ∼ 0.1 MK, hence the features appear bright. The 193 Å also has the same peak, but the filter has a broad temperature range so can also have significant contribution from plasma with $0.2 < T < 10$ MK. Hence, the emission from the hotter coronal plasma is dominant in 193 Å which would lead to a weaker signal of a $T \sim 0.1 - 0.2$ MK plasma in the channel.

3.2. Periods in faint emission

Now, let us investigate the nature of the oscillatory phenomena with period > 50 s which had significant power in the wavelets

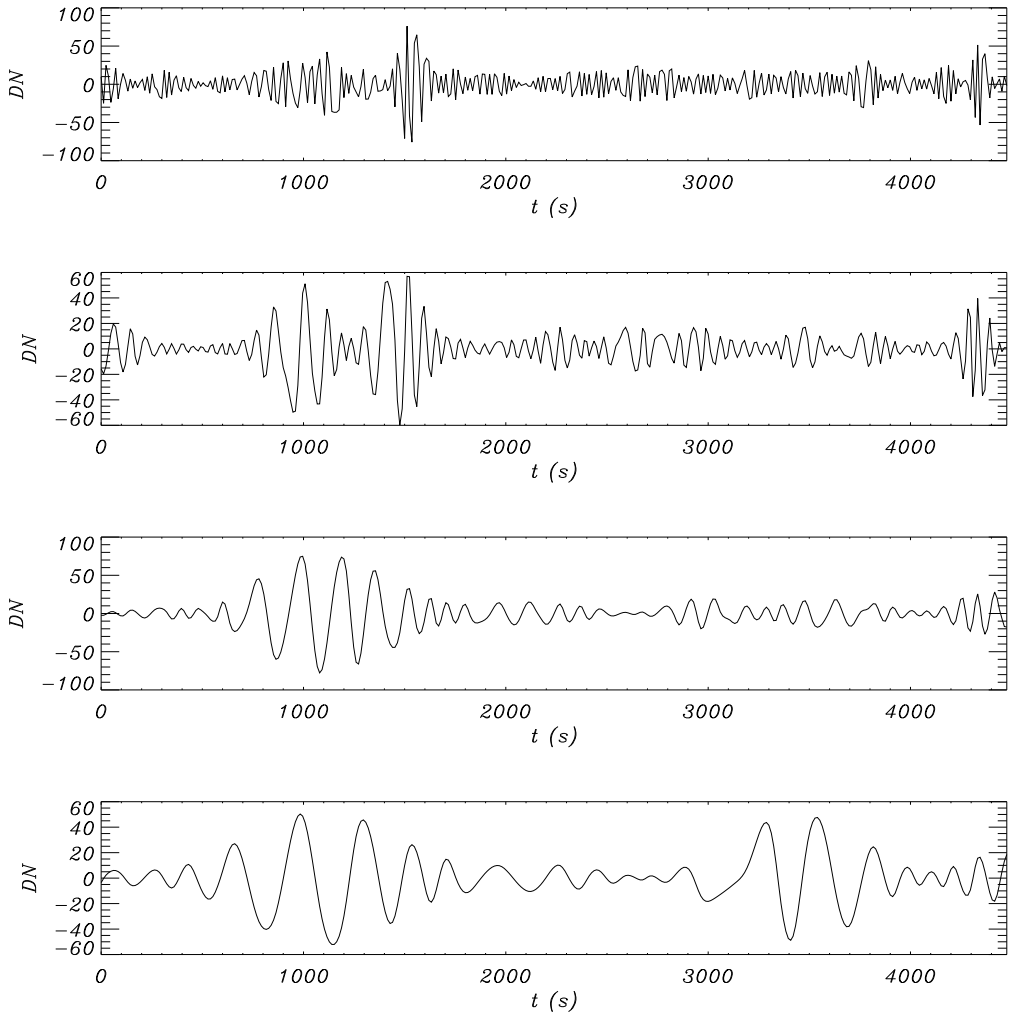

Fig. 10: The first four Intrinsic modes functions obtained using Empirical mode decomposition. From top to bottom, the panels correspond to characteristic time scales of 50 s, 100 s, 200 s and 300 s.

(Fig. 8 and 9). We ignore the 500 s period, as this begins well before and ends after the large jet, and concentrate our attention on the 300 s period phenomena which is found in the wavelets of the intensity time series from both channels. It can be seen from the wavelets (Fig. 8 and 9) and EMD (Fig. 10) that the 300 s oscillatory signal starts at around 750 s, which is before we see the periodic ejection of hot plasma (1400 s). At this time in the 304 Å channel, three to four small bright flashes are detected in the region where the jet will appear from. The bright loop/arcade, mentioned earlier, then appears ∼ 100 s later in the same region. Watching the movie supplied online (http://www.shef.ac.uk/....), it can be seen that waves begin to propagate from the region which the jet will emerge and along the open field lines which the jet will follow. However, the amplitude of the wave decreases with height and disappears from view at around 18 Mm above the surface. Once the jet appears from the surface (corresponding to the first large peak in the time series at ∼ 1000 s) the amplitude of the 300 s oscillation increases significantly and the signal is seen to propagate much higher into the atmosphere, to around 100 Mm. The larger amplitude signal seems to follow the helical path the plasma curtain takes.

As mentioned, the natural interpretation for a strong periodic modulation of intensity is the slow MHD wave. Due to the fact we observe no up-flowing material when the initial 300 s oscillation begins, we conclude it is probably not due to ejected plasma. Once the jet begins, the modulation of the intensity could be due to up-flowing material. We will discuss this further in Section 4.

If we now take the FFT for each pixel in the cross-cut 2 and use a Gaussian filter centered on 300 s with a width $f/10$ and take the inverse FFT, we obtain a filtered time series for each pixel. The results are plotted in Fig. 12 for 171 Å and Fig. 13 for 304 Å, where it can be seen that the oscillation propagates along the cross-cut. The measured speed of the oscillation, after 1000 s is 35 ± 5 kms^{-1}. Assuming we are detecting an intensity oscillation due to the the slow mode, we can use magneto-seismology to estimate the temperature of the plasma supporting the oscillation. The phase speed for the slow mode is given approximately by the sound speed $c_s = \sqrt{RT}$, where R is the ideal gas constant. This means the initial temperature of the plasma is 0.15 ± 0.05 MK. Both channels are sensitive to this range, although this is close to the peak sensitivity in 304 Å and to the cutoff temperature for the 171 Å. The wavelet analysis of the in-

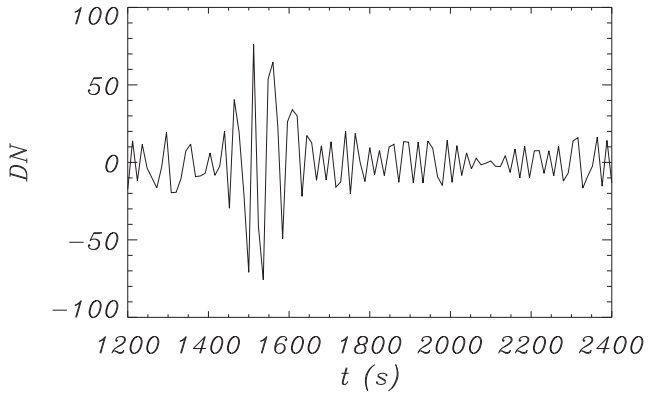

Fig. 11: Zoom of the first IMF shown in Fig. 10 to highlight the 50 s period, damped oscillation in the bright emission.

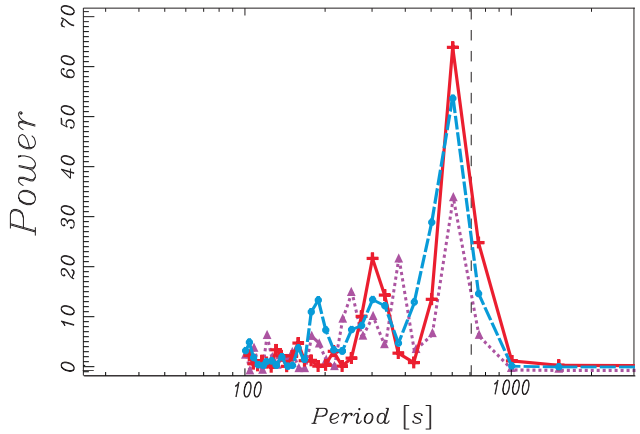

Fig. 14: Comparison of Fourier power derived from wavelet routine. The power series are derived from the intensity time series for 304 Å, 171 Å and 131 Å shown in red (solid line and crosses), blue (dash and circles) and purple (dot and triangles), respectively.

tensity time series for individual pixels in 131 Å cross-cut do not show significant power at 300 s, which is would be expected if the signal is connected to plasma with $T < 0.2$ MK. This oscillation appears to reside in the bulk of the up-flowing plasma which dominates the observation in 304 Å, i.e. the plasma curtain, and can be faintly seen in 171 Å. Comparing the Fourier power spectra derived from the wavelets, in Fig. 14 it can be seen that the power of the oscillation is stronger in the 304 Å channel with decreasing power in the 171 Å and 131 Å channels. This gives further credence to the estimation of the temperature from the seismology.

Finally, we come onto the 200 s period oscillation observed only in the 171 Å transform. We again perform an FFT and apply a Gaussian filter about 200 s for each pixel in the cross-cut (results shown in middle panel of Fig. 12). We find the propagation speed of the oscillation along the cross-cut is $\sim 23 \pm 5$ kms^{-1}. If we assume the intensity modulation is, again, due to the slow mode then this gives the temperature of the plasma supporting the oscillation as $T \sim 4 - 9 \times 10^4$ K. The calculated temperature of the plasma is close to the bottom end of the range of temperature which the 171 Å channel is sensitive too. However, if we look at the times at which the 200 s oscillation begins, it is at the same time as the dark feature passes through the cross-cut. The dark features rise speed along the cross-cut is also ~ 23 kms^{-1} (the actual rise velocity is ~ 60 kms^{-1}, see Morton et al., 2011b). It would appear as if the passage of the dark feature through the cross-cut is the cause of the oscillation. This is confirmed as we find a velocity of ~ 16 kms^{-1} for the dark thread in the cross-cut 1 and the 200 s oscillation also has a propagation velocity of 16 kms^{-1}. The cross-cuts along the bright features are located at an angle to the path the dark filament is ejected along, hence we obtain rise speeds a fraction of that reported in Morton et al. (2011b). If the dark filament is the driver for the oscillation then its actual propagation speed could also be $\sim 60 - 70$ kms^{-1}. Placing a cross-cut along the filaments axis, almost perpendicular to the solar surface (see, e.g. the filament in Fig. 1e) we obtain propagation speeds of the order 60 kms^{-1} for the 200 s oscillation.

4. Discussion

High-speed up-flows in large solar jets have been reported previously by Liu et al. (2009) and Sterling et al. (2010), although no periodicity was detected in the up-flow. The properties of the high-speed up-flows that are observed here also bring to mind recent results of investigations into type-II spicules (e.g. De Pontieu et al., 2007a). It is thought that reconnection drives the type-II spicules which are characterised by the ejection high velocity up-flows ($\sim 40 - 120$ kms^{-1}) of hot material into the corona (De Pontieu et al., 2011). The emission is seen to originate in the chromosphere with temperatures of $\lesssim 0.1$ MK and velocities of ~ 40 kms^{-1}, before appearing in coronal lines with temperatures of > 1 MK and velocities of ~ 120 kms^{-1}. The presence of type-II spicule-like events in large jets was discussed in Sterling et al., 2010. As pointed out by the authors, the type-II spicule-like features are part of the macroscopic jet so the situation is somewhat more complicated than individual type-II spicules.

Such a statement is highlighted with the following differences between the spicule-like events we see here and previously reported type-II spicules. The bright, fast moving features we observe here have a period of reoccurrence of the order of 50 s, while previous reports indicate periods of $5 - 12$ minutes for type-II spicules (De Pontieu & McIntosh, 2010). However, this would indicate a difference between the recurrence rate of the drivers of the events. A further difference is that the periodic behaviour observed here displays damping and apparently only lasts for 5 periods, whereas no such features have been reported with type-II spicules previously, to our knowledge.

How can we explain such an oscillatory phenomena in terms of the suggested mechanisms of jet formation? One option is that there are multiple reconnection events between emerging, closed field lines and open field lines, causing the numerous ejections which are being guided upwards by the open field lines. The data also suggests that the reconnection event would probably have to be periodic or quasi-periodic. This has been demonstrated to be possible in 2-d models if the reconnection has been driven by a fast magnetoacoustic wave (McLaughlin et al., 2010). If

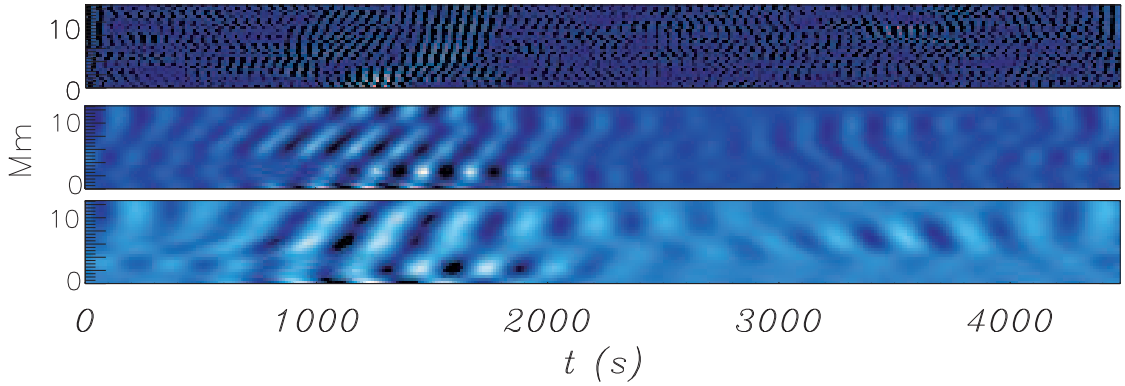

Fig. 12: Frequency filtered time series obtained from the 171 Å cross-cut 2 shown in Fig. 4. The top, middle and bottom rows are filtered at 50 s, 200 s and 300 s, respectively.

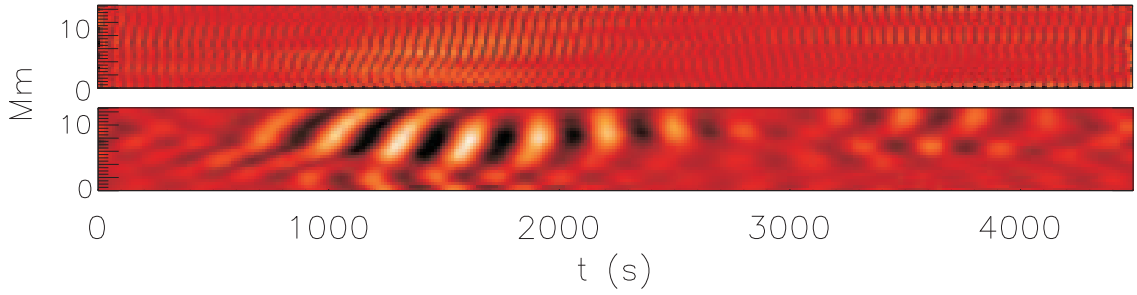

Fig. 13: Frequency filtered time series obtained from the 304 Å cross-cut 2 shown in Fig. 4. The top and bottom rows are filtered at 50 s and 300 s, respectively.

this event is reconnection driven, then the multi-ejections provide evidence for 'nano-flare') storms. The 'nano-flare' storms are usually associated with heating of active region loops (e.g., Klimchuk et al., 2010) but it is plausible that they could be responsible for the heating and mass supply of many different plasma features. The multiple reconnection events would only constitute a short 'nano-flare'storm, lasting for only 300 s.

Another possibility is that only one reconnection event has occurred and we are seeing the response of the transition region to a single velocity pulse. The rebound-shock model suggests that a velocity pulse can cause the transition region to generate a periodic response (Hollweg et al., 1982; Murawski & Zaqarashvili, 2010). However, the bright, fast moving emission can be seen up to heights of at least 18 arcseconds (12 Mm). Simulations of spicule formation via waves show that wave driven spicule phenomena cannot reach such heights (for a review, see, e.g., Sterling, 2000). Although, typical amplitudes and velocities for these simulations are based on driving by photospheric granulation, so the results may not be directly applicable here if reconnection driven outflows are the driver.

The oscillation with the period of 300 s appears to be different from the periodic behaviour associated with the type-II spicule-like like events. The propagation of 300 s period waves into the atmosphere starts after multiple bright events are seen in the region which the jet appears from. This would suggest that whatever physical process in the chromosphere is responsible for the large jet, aides and enhances the propagation of 300 s oscillations (known to be present throughout the solar atmosphere see, e.g. Banerjee et al., 2007) into the corona or is a driver for slow magneto-acoustic waves.

The larger amplitude 300 s intensity oscillations are present as the jet is erupting and seems to be related to the plasma curtain that makes up the visible jet in 304 Å. After studying the data, we find no direct evidence for any mechanism that could excite the 300 s oscillation. It could be the excitation mechanism happens low in the chromosphere and is not visible to SDO/AIA, such as generation of slow shocks at the reconnection site (e.g. Yokoyama & Shibata, 1996). Another possible explanation is that the periodic behaviour is caused by the rebound-shock reaction of the transition region (Hollweg et al., 1982). There maybe some difficulty with this explanation if we assume the 300 s oscillation is a signature for a mechanism that is pumping mass from the chromosphere into the corona, as simulations have shown wave-based mechanisms cannot eject material to great heights, e.g., the simulation of small chromospheric jets such as spicules (De Pontieu et al., 2004), fibrils (Hansteen et al., 2006), mottles (Heggland et al., 2007)) typically have heights < 5 Mm. Although, as mentioned before, such models are based on photospheric drivers which have small amplitudes (i.e., $\sim$ 1 kms^{-1} for granular motions). Large amplitude (i.e. non-linear) waves driven by the reconnection event may provide different results.

There is also the presence of a 200 s oscillation in the 171 Å time series. The oscillation appears to be driven by the passage of the cool filament. The signal for the oscillations is strong close the jet footpoints but appears to decay with height and

does not propagate high into the atmosphere (see online movie). One possibility for its existence is that the passage of the filament through the transition region results in the initiation of the rebound-shock process, causing the periodic signal.

5. Summary and Conclusions

We study a large solar jet event that occurs close to the southern polar coronal hole. Due to a number of observational signatures such as a loop/arcade brightening, an untwisting field and the final height of the large jet we conclude that the jet is probably initiated by a magnetic reconnection event between a twisted, closed field and an open magnetic field. The presence of plasma with temperatures from 0.02 MK to 0.2 MK suggest this event falls into the blowout jet scenario (Moore et al., 2010), although no high temperature (X-ray) component is observed. To investigate the process of jet formation we take a novel approach and look for periodic behaviour present in the jet.

Multiple bright, fast moving ($40 - 150 \mathrm{kms}^{-1}$) plasma ejections are observed and have properties that are similar to those reported for type-II spicules (De Pontieu et al., 2007b). Interpretation of the observed events as type-II spicule-like features is not incompatible with the idea that a reconnection based mechanism is responsible for generating the large solar jets. The events appear to have a period of 50 s, suggesting that periodic reconnection may be occurring. Such a collection of rapidly occurring reconnection events appears to provide evidence for small 'nano-flare' storms.

On the other hand, the faint plasma emission has a longer period oscillation with a period of 300 s. The oscillation had significant power in the 304 Å and 171 Å channels and was found to propagate along the slits at 36 kms^{-1}. Assuming it is a slow magnetoacoustic mode, the inversion of the propagation speed gives a plasma temperature of 0.1 MK. We suggest this connects the 300 s oscillation with the bulk of plasma that appears to makes up the jet in 304 Å.

In our view, the presence of the multiple bright, fast moving plasma ejections here, and in previous works (Sterling et al., 2010), suggests that type-II spicule-like events could play an important role in determining the appearance of the jets. Type-II events are already thought to be important for maintaining the mass balance in the corona (e.g., McIntosh & De Pontieu, 2009b, McIntosh & De Pontieu, 2009a) and could be important for the distribution of the UV/EUV temperature material, that makes up the larger jet, into the corona. The extent of the role played by the response of the transition region to waves and flows impinging on it also needs further detailed study.

Acknowledgements. The authors thank A. Engell, D. Jess, and P. Grigis for a number of useful discussions. RE acknowledges M. Kéray for patient encouragement. The authors are also grateful to NSF, Hungary (OTKA, Ref. No. K83133) and the Science and Technology Facilities Council (STFC), UK for the financial support they received. AKS thanks SP^2RC for the financial support received for the visits and collaborative research. The data is provided courtesy of NASA/SDO and the AIA, EVE, and HMI science teams.

References

Andries, J., van Doorsselaere, T., Roberts, B., et al. 2009, Space Science Reviews, 149, 3
Banerjee, D., Erdélyi, R., Oliver, R., & O'Shea, E. 2007, Sol. Phys., 246, 3
Beckers, J. M. 1972, ARA&A, 10, 73
Bohlin, J. D., Vogel, S. N., Purcell, J. D., et al. 1975, ApJ, 197, L133
Brueckner, G. E. & Bartoe, J. 1983, ApJ, 272, 329
Budnik, F., Schroeder, K., Wilhelm, K., & Glassmeier, K. 1998, A&A, 334, L77
Cirtain, J. W., Golub, L., Lundquist, L., et al. 2007, Science, 318, 1580
Curdt, W. & Tian, H. 2011, A&A, 532, L9+
De Moortel, I. 2009, Space Science Reviews, 149, 65
De Pontieu, B., Erdélyi, R., & James, S. P. 2004, Nature, 430, 536
De Pontieu, B., McIntosh, S., Hansteen, V. H., et al. 2007a, PASJ, 59, 655
De Pontieu, B. & McIntosh, S. W. 2010, ApJ, 722, 1013
De Pontieu, B., McIntosh, S. W., Carlsson, M., et al. 2011, Science, 331, 55
De Pontieu, B., McIntosh, S. W., Carlsson, M., et al. 2007b, Science, 318, 1574
De Pontieu, B., McIntosh, S. W., Hansteen, V. H., & Schrijver, C. J. 2009, ApJ, 701, L1
Erdélyi, R. 2006a, Royal Society of London Philosophical Transactions Series A, 364, 351
Erdélyi, R. 2006b, in Proceedings of SOHO 18/GONG 2006/HELAS I, Beyond the spherical Sun, ed. K. Fletcher & M. Thompson, ESA SP-624
Hansteen, V. H., De Pontieu, B., Rouppe van der Voort, L., van Noort, M., & Carlsson, M. 2006, ApJ, 647, L73
He, J., Marsch, E., Tu, C., & Tian, H. 2009, ApJ, 705, L217
Heggland, L., De Pontieu, B., & Hansteen, V. H. 2007, ApJ, 666, 1277
Hollweg, J. V., Jackson, S., & Galloway, D. 1982, Sol. Phys., 75, 35
Huang, N. E., Shen, Z., Long, S. R., et al. 1998, Royal Society of London Proceedings Series A, 454, 903
Jess, D. B., Mathioudakis, M., Erdélyi, R., et al. 2009, Science, 323, 1582
Kamio, S., Curdt, W., Teriaca, L., Inhester, B., & Solanki, S. K. 2010, A&A, 510, L1+
Klimchuk, J. A., Karpen, J. T., & Antiochos, S. K. 2010, ApJ, 714, 1239
Kukhianidze, V., Zaqarashvili, T. V., & Khutsishvili, E. 2006, A&A, 449, L35
Lemen, J. R., Title, A. M., Akin, D. J., et al. 2011, Sol. Phys., 115
Liu, W., Berger, T. E., Title, A. M., & Tarbell, T. D. 2009, ApJ, 707, L37
Liu, W., Berger, T. E., Title, A. M., Tarbell, T. D., & Low, B. C. 2011, ApJ, 728, 103
Martínez-Sykora, J., Hansteen, V., & Moreno-Insertis, F. 2011, ApJ, 736, 9
McIntosh, S. W. & De Pontieu, B. 2009a, ApJ, 707, 524
McIntosh, S. W. & De Pontieu, B. 2009b, ApJ, 706, L80
McLaughlin, J. A., Hood, A. W., & de Moortel, I. 2010, Space Sci. Rev., 62
Moore, R. L., Cirtain, J. W., Sterling, A. C., & Falconer, D. A. 2010, ApJ, 720, 757
Moore, R. L., Sterling, A. C., Cirtain, J. W., & Falconer, D. A. 2011, ApJ, 731, L18+
Morton, R. J., Erdélyi, R., Jess, D. B., & Mathioudakis, M. 2011a, ApJ, 729, L18
Morton, R. J., Verth, G., McLaughlin, J. A., & Erdélyi, R. 2011b, ApJ
Murawski, K. & Zaqarashvili, T. V. 2010, A&A, 519, A8
Newton, H. W. 1934, MNRAS, 94, 472
Pariat, E., Antiochos, S. K., & DeVore, C. R. 2009, ApJ, 691, 61
Patsourakos, S., Pariat, E., Vourlidas, A., Antiochos, S. K., & Wuelser, J. P. 2008, ApJ, 680, L73
Pike, C. D. & Mason, H. E. 1998, Sol. Phys., 182, 333
Roberts, B., Edwin, P. M., & Benz, A. O. 1984, ApJ, 279, 857
Ruderman, M. S. & Erdélyi, R. 2009, Space Science Reviews, 149, 199
Schrijver, C. J., Title, A. M., Harvey, K. L., et al. 1998, Nature, 394, 152
Scullion, E., Erdélyi, R., Fedun, V., & Doyle, J. 2011, Submitted
Secchi, P. A. 1877, La Soleil, Vol. 2, Chapter II (Paris: Gauthier-Villars)
Shibata, K., Ishido, Y., Acton, L. W., et al. 1992, PASJ, 44, L173
Shibata, K., Nakamura, T., Matsumoto, T., et al. 2007, Science, 318, 1591
Shibata, K. & Uchida, Y. 1985, PASJ, 37, 31
Shimojo, M., Hashimoto, S., Shibata, K., et al. 1996, PASJ, 48, 123
Sterling, A. C. 2000, Sol. Phys., 196, 79
Sterling, A. C., Harra, L. K., & Moore, R. L. 2010, ApJ, 722, 1644
Taroyan, Y. & Erdélyi, R. 2009, Space Science Reviews, 24
Terradas, J., Oliver, R., & Ballester, J. L. 2004, ApJ, 614, 435
Tian, H., McIntosh, S. W., & De Pontieu, B. 2011, ApJ, 727, L37+
Uchida, Y. 1970, PASJ, 22, 341
Vasheghani Farahani, S., Van Doorsselaere, T., Verwichte, E., & Nakariakov, V. M. 2009, A&A, 498, L29
Verwichte, E., Marsh, M., Foullon, C., et al. 2010, ApJ, 724, L194
Wang, T. 2011, Space Sci. Rev., 16
Wang, T., Ofman, L., & Davila, J. M. 2011, ArXiv e-prints
Yokoyama, T. & Shibata, K. 1995, Nature, 375, 42
Yokoyama, T. & Shibata, K. 1996, PASJ, 48, 353
Zaqarashvili, T. V. & Erdélyi, R. 2009, Space Sci. Rev., 149, 355